Aptasensor Based on Screen-Printed Carbon Electrodes Modified with Aunps/CS for Sensitive Detection of Okadaic Acid in Shellfish

Yiyang Dong (yydong@mail.buct.edu.cn)
Beijing University of Chemical Technology https://orcid.org/0000-0003-1752-3935
Ni Zeng
Beijing University of Chemical Technology
Yan Yang
Beijing University of Chemical Technology
Yingai Yin
Beijing University of Chemical Technology
Lianhui Zhao
Beijing University of Chemical Technology
Xu Wang
Beijing University of Chemical Technology

Research Article

Keywords: okadaic acid, aptasensor, screen-printed carbon electrode, chitosan, gold nanoparticles, cyclic voltammetry

Posted Date: March 8th, 2022

DOI: https://doi.org/10.21203/rs.3.rs-1347006/v1

Abstract

Objective

Based on the specific binding of target with aptamer, a portable aptasensor combined with highly sensitive electrochemical methods was designed to complete the rapid detection of biological toxins Okadaic acid (OA) in shellfish.

Results

A simple aptasensor based on screen-printed carbon electrode (SPCE) with modification of chitosan (CS) and gold nanoparticles (AuNPs) was designed for electrochemical determination of OA, and the electrode surface was modified with AuNPs by potential-sweeping electrodeposition, which greatly improved the electrochemical response. The entire detection and characterization process were carried out by cyclic voltammetry (CV) with a linear correlation in the range from 0.01 ng/mL to 100 ng/mL and a LOD of 6.7 pg/mL. Furthermore, a recovery rate of 92.30-115.98% was obtained demonstrating excellent accuracy through the recovery trial of mussel and scallop samples.

Conclusion

The current method based the change of spatial structure before and after aptamer binding target showed great potential in rapid on-site and low-cost detection of OA for its simplicity.

Introduction

According to the clinic symptoms caused by seafood consumption, Okadaic acid (OA), a typical diarrhetic shellfish poisoning (DSP) toxin, is a small molecular polyether compound(Fu et al. 2019), and could accumulate in the shellfish's digestive glands when the toxic microalgae is filtered and ingested by the bivalve shellfish. OA not only will cause poisoning symptoms such as diarrhea and vomiting after accidental ingestion of poisoned shellfish, but also can induce cancer as a tumor promoter with a long-term shellfish consumption(Jimenez-Carcamo et al. 2020; Kong et al. 2020). According to the current EU regulations, the content of OA in the edible tissues of bivalve molluscs shall not exceed 160 μg/kg(Anon. 2004).

As standard or officially accrediated methods to quantitatively detect OA, mouse bioassays(Suzuki et al. 2018), high performance liquid chromatography (HPLC)(Yamaguchi M et al. 2016) and so on are generally limited in reality because of ethical issues, expensive equipment, cumbersome steps, and high operational requirements. For that, more and more innovative technologies have been developed during the past decades, such as electrochemical sensor technology(Eissa et al. 2013),

electrochemiluminescence technology(Yang et al. 2021) and immunology sensing technology(Antunes et al. 2018).

Amongst aforementioned methods, electrochemical sensing technology has been widely used due to its low cost and high sensitivity, of which aptamers that can specifically bind to the target are often used as biological recognition elements for detection(Ye et al. 2019; Zhao et al. 2021). Aside from technological breakthroughs, some quick detection researches based on aptasensors with composite materials(Peng et al. 2020; Verma et al. 2020) and modification of aptamer structures(Chinnappan et al. 2019) are also emerging. However, the preliminary preparation process of these methods is too cumbersome and has a direct impact on the final signal response. Simultaneously, pre-experiments for aptamer modification must be carried out in advance, including optimization of sequence length and modification sites through molecular docking and related analyses. Furthermore, when aptamers are labeled with fluorescent or electroactive molecules to improve the electrochemical response or expand the application, the costs of corresponding raw detection material or element rise, and the labeling quality is likely to have a negative impact on final detection.

This study aimed to improve the simplicity of the construction process of aptasensor under the premise of meeting the rapid testing requirements, and make up for the problem of low response signal of carbon electrode by using the double modification of chitosan and gold nanoparticles. The use of disposable screen-printed electrode avoided cross pollution and the complex pretreatment process, which achieved the purpose of miniaturized and rapid detection of okadaic acid in actual sample.

Experimental Section

Materials

OA was purchased from MedChemExpress (Wuhan, China). And the aptamer sequences (OA34) specific to Okadaic acid were identified from previous studies(Eissa et al. 2013) and synthesized by Sangon Biotech (Shanghai, China). The sequence of 5'- C6- thiolated OA34 is as follows:

5'-C6-SH-GGTCACCAACAACAGGGAGCGCTACGCGAAGGGTCAATGT GACGTCATGCGGATGTGTGG-3'

The mussels and scallop samples used in the experiment were purchased from local store in Lianyungang, Jiangsu in May 2021, and were OA negative by the LC-MS/MS method.

Instrumentation

Electrochemical measurements were carried out on the BDT mini STAT 100 electrochemistry system (Bio Device Technology, Japan). And the three-electrode system used in this work consisting of a carbon working electrode, a carbon auxiliary electrode and an Ag/AgCl reference electrode was purchased from

the same company. Scanning electron micrographs (SEM) of the morphology of the electrode surface were obtained with a scanning electron microscope (TESCAN, China).

Preparation of AuNPs/CS modified electrode

To obtain the AuNPs/CS/SPCE, 2 uL 4 mg/mL CS solution was dropped on the SPCE surface and air-dried at room temperature, then submerged in 50 uL 5 mM HAuCl4 solution and modified with AuNPs by potential-sweeping electrodeposition using a cyclic voltammetry scanning between -0.6 V and 1.2 V at a scan rate of 50 mV/s.

Preparation of OA aptasensor

To begin this process, the thiolated OA34 dissolved in binding buffer (50 mM Tris, pH 7.5, 150 mM NaCl, 2 mM $MgCl_2$)(Eissa et al. 2013) should be placed in a metal bath at 95 °C for 5 min to maintain its original conformation before being completely reduced with 10 mM TCEP for 1 h. Then the AuNPs/CS/SPCE was functionalized by self-assembling with forming Au-S bonds in a 20 μL aptamer solution overnight. After that, the electrode was incubated in 50 μL 1 mM 6- mercapto- 1- hexanol (MCH) for 1 h. The modified electrode was then completely washed with ultrapure water and employed in electrochemical experiments right away, or stored in binding buffer solution at 4 °C for subsequent use.

Electrochemical measurements

All electrochemical measurements were recorded in a 10 mM PBS buffer solution containing 5 mM $[Fe(CN)_6]^{3-/4-}$ redox pair (1:1 molar ratio) and 100 mM KCl, then performed by cyclic voltammetry (CV) with a potential sweeping between -0.4 V and 0.7 V. The scan rate was set at 100 mV/s and the number of repeat times was set to 5. Unless otherwise stated, all electrochemical measurements were taken as above.

Detection of OA in real samples

The shellfish meat was drained by a metal sieve with an aperture of about 2 mm for 5 min, then cut into pieces. Next 2 g shellfish pieces were mixed with 9 mL methanol for 1 min and centrifugated at 8000 rpm for 5 min. Furthermore, the supernatant was isolated into a fresh centrifuge tube, and 9 mL methanol was added to mix the precipitation again. After the same process, the obtained supernatant was mixed and diluted to 20 mL with methanol to be the extract. Next 1 mL extract was incubated with 125 μL 2.5 mol/L sodium hydroxide solution for 40 min at 76 ℃, and cooled to room temperature. Then the solution was neutralized with 125 μL 2.5 mol/L hydrochloric acid. Finally, the obtained hydrolysate (1.25 mL was equivalent to 0.1 g sample) was dealt with nitrogen blow to near dryness after directly passing through a

0.22 μM organic phase microporous membrane, and re-dissolved in 1 mL binding buffer for ultimate detection.

Results And Discussion

Principle of the assay

The electrochemical detection of OA was demonstrated in Fig. 1. As the recognition element, the aptamer OA34 was immobilized on the electrode surface by self-assembling with AuNPs, and its directional arrangement was achieved following treatment with MCH, making adaptive folding and binding with targets easier. After binding with OA, the alteration of the aptamer conformation from loose to tight caused a substantial increase in the electron-transfer current as measured by CV, and the quantitative detection of OA can be completed by establishing the relationship between them.

(The position of Fig. 1)

The optimization of modified condition and the characterization of AuNPs/CS/SPCE

To improve the electrochemical response as much as possible, the relevant conditions of modification with CS and AuNPs were optimized in this study.

The increase in peak currents can be attributed to the conductivity of CS obviously, but a possible explanation for the decrease might be that the film formed by excess CS layers was so thick that the charge transfer was inhibited (Fig. 2 A).

The reduction peak currents increased obviously with the increase in scan cycles (equivalent to deposition time) at the beginning and tended to stabilize after 5 cycles because of the limited electrodes surface area. To bind as much aptamers as possible on electrodes, 6 cycles were adopted to deposit AuNPs (Fig. 2 B).

(The position of Fig. 2)

After the modification with CS and AuNPs, SEM was used to characterize the different morphologies of SPCE, CS/SPCE and AuNPs/CS/SPCE. The SPCE working surface consisted of lots of irregular and blocky structure (Fig. 3 A), and there was little significant difference with drip-coated CS (Fig. 3 B). Then the surface was obviously attached with uniform and dense particles additionally after deposition (Fig. 3 C), which could be inferred that AuNPs had been modified successfully on the surface of electrode with an average particle size less than 100 nm. Furthermore, the CV curves recorded in 0.2 M sulfuric acid (Fig. 3 D) performed a reduction peak current corresponded to the potential about 0.4 V, which ment the characteristic reduction peak of Au.

(The position of Fig. 3)

Feasibility of the method and the optimization of experimental condition

The electrochemical behaviors of different modification processes were characterized by CV. Fig. 4 (A) showed that the SPCE without any modification exhibited low redox peak currents (curve a). After modification with drip-coated CS and AuNPs by electrodeposition on the surface, the currents increased about 7 μA because of the good conductivity of CS and AuNPs (curve b). While the currents decreased evidently with incubation in aptamers solution overnight (curve c), which proved that the aptamers had been immobilized on the electrode successfully. Then the currents decreased even further after the blocking of the nonspecific sites with MCH (curve d). Finally, the incubation of OA increased the currents due to the specific binding of aptamers and targets (curve e).

In this work, considering the sensitivity and nonspecific adsorption of the sensor, we optimized the aptamer concentration, MCH blocking time and target incubation time respectively to achieve the best detection conditions, which were selected according to the reduction peak currents differences before and after operation. Fig. 3 (B, C and D) showed the signal differences of reduction peak current (Δi_p), and the optimal setting values of these three parameters were finally determined as 10 μM, 60 min and 60 min.

(The position of Fig. 4)

Analytical Performance, stability and selectivity of the aptasensor

The sensor response to OA concentrations ranging from 0.001 ng/mL to 100 ng/mL was measured with the above-mentioned optimal conditions (Fig. 5 A). The change of the reduction peak current as per the aptamer conformation upon binding with OA was observed clearly by the reduction percentage ($\Delta i_p / i_{p,0}$) (where the $i_{p,0}$ was the reduction peak current before the binding of the aptasensor with OA) of signal here. The data points in the calibration curve represented three independent measurements. In order to intuitively show aptasensor response to OA concentrations, the curve was displayed with the reduction percentage of reduction peak currents to the logarithmic values of the OA concentrations. And there was a linear increase of the signal with the concentrations changing from 0.01 ng/mL to 100 ng/mL ($y= 6.70303 +1.13752*x$, $R^2 = 0.99877$, where x was the logarithmic value of the OA concentration, and y was the reduction percentage of the reduction peak current before and after binding with OA). The limit of detection (LOD) of the biosensor was calculated to be about 6.7 pg/mL (S/N=3), which was better than or comparable to some of the previously reported electrochemical and other aptasensors.

In this work, the stability of the sensor was confirmed by inter-day trials for five continuous days. The peak currents after combining the sensor with 10 ng/mL OA were measured by CV (Fig. 5 B). During the scanning process, the reduction peak currents ($i_{p,r}$) were always slightly higher than the oxidation peak currents ($i_{p,o}$). And there was no significant difference both of them for five consecutive days, indicating the good stability of this method.

(The position of Fig. 5)

Analysis of Real Samples

In this work, the relevant extracts were obtained from fresh mussel and scallop samples by the sample processing steps described in the methods section. The extracts spiked with different known concentrations including 1, 50, 100 ng/mL of OA was tested using the constructed aptasensor. And the recovery statistics for each of the samples examined was shown in Table.1, ranging from 92.30 % to 115.98 % for an average of n = 3 replicates with an RSD from 8.64 % to 17.28 %, which represented a good performance in real samples.

Conclusion

In summary, an electrocheimcal aptasensor based on SPCE was developed for the detection of OA in shellfish. In this method, the quantitative detection of OA was obtained with the charge transfer difference caused by the change of spatial structure before and after aptamer binding with the targets. The electrochemical performance of the aptasensor was dramatically enhanced with sequential modifications of CS and AuNPs, which decreased the inherent discrepancies of the screen-printed gold electrodes to a favorable extent. And there was no special structural modification or electroactive molecular labeling of the aptamer, lowering the cost of raw materials while meeting the detection requirements. Compared with other sensors, this method could be employed as a new and portable type of rapid detection scheme for daily monitoring and field detection of OA in shellfish with ease.

Declarations

Acknowledgment

This work was supported by Beijing University of Chemical Technology-China-Japan Friendship Hospital Biomedical Translation Engineering Research Center Joint Project (RZ2020-02) and the National Key Research and Development Program of China (2016YFF0203703).

Conflict of interest All the authors declare that there is nocompeting interest.

References

1. Anon. (2004). Regulation (EC) No. 853/2004 of the European Parliament and of the Council of 29 April 2004 laying down specific hygiene rules for food of animal origin.
2. Antunes, J., Justino, C., da Costa, J. P., Cardoso, S., Duarte, A. C., & Rocha-Santos, T. (2018). Graphene immunosensors for okadaic acid detection in seawater. *Microchemical Journal, 138*, 465-471.
3. Chinnappan, R., AlZabn, R., Mir, T. A., Bader, M., & Zourob, M. (2019). Fluorometric determination of okadaic acid using a truncated aptamer. *Mikrochim Acta, 186*(7), 406.
4. Eissa, S., Ng, A., Siaj, M., Tavares, A. C., & Zourob, M. (2013). Selection and identification of DNA aptamers against okadaic acid for biosensing application. *Anal Chem, 85*(24), 11794-11801.
5. Fu, L. L., Zhao, X. Y., Ji, L. D., & Xu, J. (2019). Okadaic acid (OA): Toxicity, detection and detoxification. *Toxicon, 160*, 1-7.
6. Jimenez-Carcamo, D., Garcia, C., & Contreras, H. R. (2020). Toxins of Okadaic Acid-Group Increase Malignant Properties in Cells of Colon Cancer. *Toxins (Basel), 12*(3).
7. Kong, J., Li, D., Zhang, S., Zhang, H., Fu, Y., Qian, B., Bei, C., Tan, S., & Zhu, X. (2020). Okadaic acid promotes epithelial-mesenchymal transition of hepatocellular carcinoma cells by inhibiting protein phosphatase 2A. *J Cell Biochem*.
8. Peng, J., Zhao, Z., Zheng, M., Su, B., Chen, X., & Chen, X. (2020). Electrochemical synthesis of phosphorus and sulfur co-doped graphene quantum dots as efficient electrochemiluminescent immunomarkers for monitoring okadaic acid. *Sensors and Actuators B: Chemical, 304*.
9. Suzuki, H., & Okada, Y. (2018). Comparative toxicity of dinophysistoxin-1 and okadaic acid in mice. *J Vet Med Sci, 80*(4), 616-619.
10. Verma, M., Chaudhary, M., Singh, A., Kaur, N., & Singh, N. (2020). Naphthalimide-gold-based nanocomposite for the ratiometric detection of okadaic acid in shellfish. *J Mater Chem B, 8*(36), 8405-8413.
11. Yamaguchi M, Yamaguchi T, Kakimoto K, Nagayoshi H, Okihashi M, & Kajimura K. (2016). Validation Study for Analytical Method of Diarrhetic Shellfish Poisons in 9 Kinds of Shellfish. *Journal of the Food Hygienic Society of Japan*.
12. Yang, W., Zhang, G., Ni, J., Wang, Q., & Lin, Z. (2021). From signal amplification to restrained background: Magnetic graphene oxide assisted homogeneous electrochemiluminescence aptasensor for highly sensitive detection of okadaic acid. *Sensors and Actuators B: Chemical, 327*.
13. Ye, W., Liu, T., Zhang, W., Zhu, M., Liu, Z., Kong, Y., & Liu, S. (2019). Marine Toxins Detection by Biosensors Based on Aptamers. *Toxins (Basel), 12*(1).
14. Zhao, Y., Li, L., Yan, X., Wang, L., Ma, R., Qi, X., Wang, S., & Mao, X. (2021). Emerging roles of the aptasensors as superior bioaffinity sensors for monitoring shellfish toxins in marine food chain. *J Hazard Mater, 421*, 126690.

Tables

Table.1 Detection of OA in real samples

Samples	Spiked Concentration (ng/mL)	Detected Concentration (ng/mL)	Recovery (%)	RSD (%)
mussels	1	0.923±0.14	92.3	15.21
	50	57.992±5.008	115.98	8.64
	100	112.296±12.072	112.3	10.75
scallops	1	0.931±0.125	93.1	13.41
	50	57.177±9.881	114.35	17.28
	100	113.839±13.941	113.84	12.25

Figures

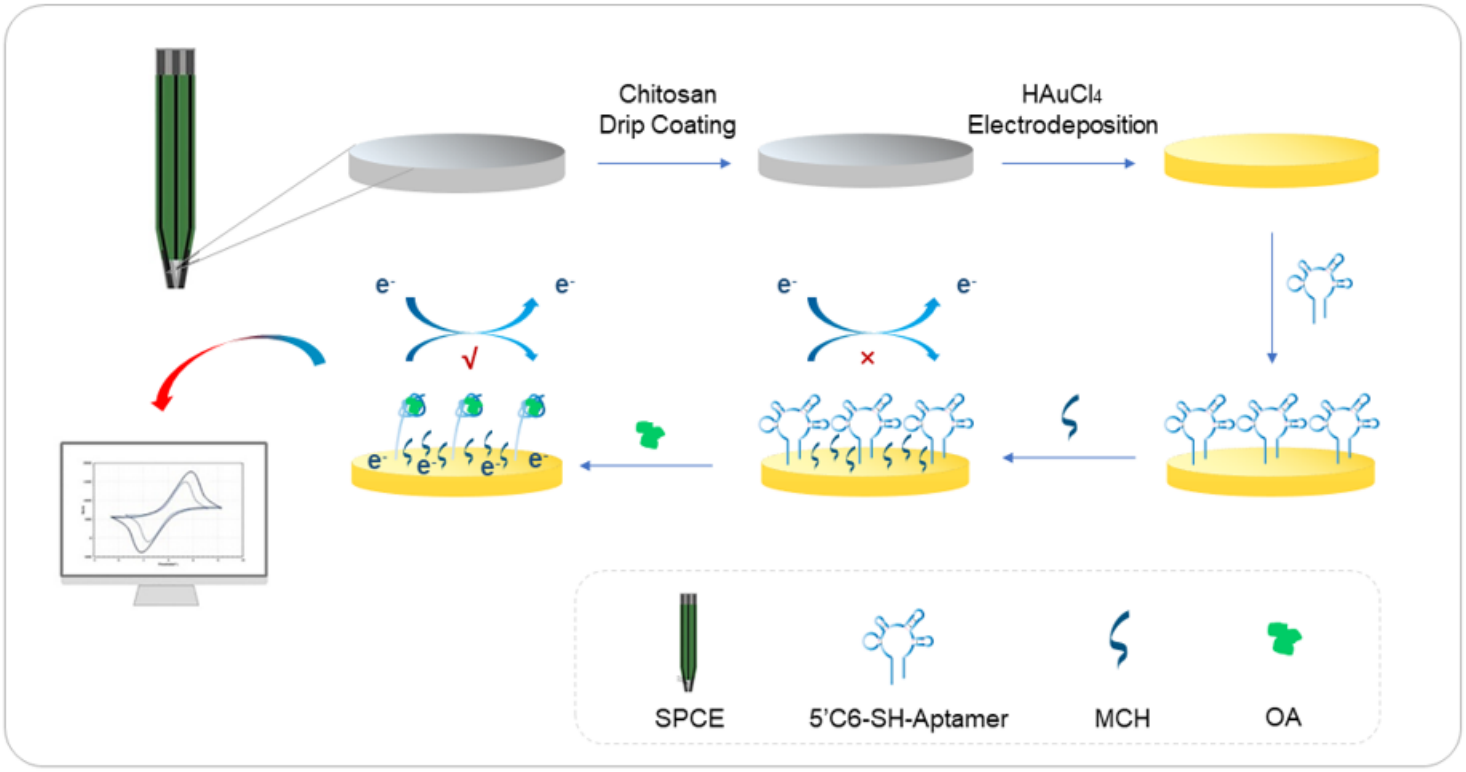

Figure 1

The schematic illustration of the electrochemical aptasensor.

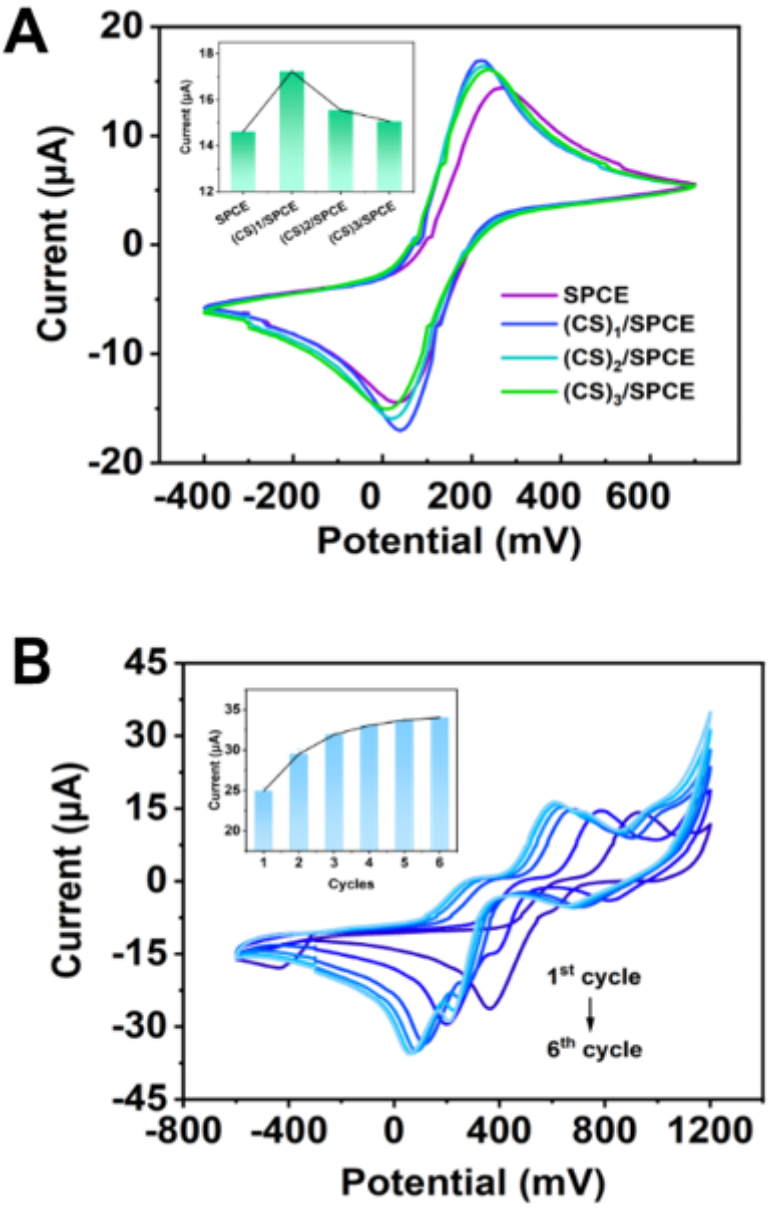

Figure 2

The CV curves of modification with drip-coated CS for 1-3 times in 5 mM $[Fe(CN)_6]^{3-/4-}$ containing 100 mM KCl (A) and electrodeposition for 1-6 cycles in 5 mM $HAuCl_4$ (B).

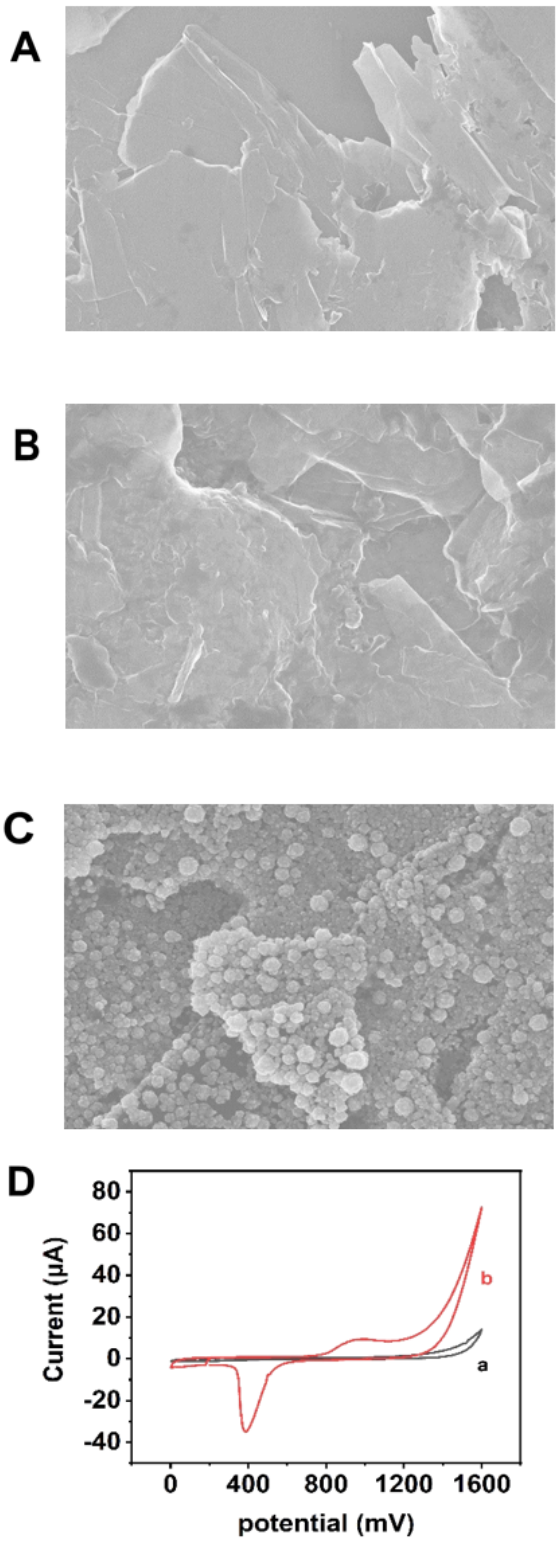

Figure 3

SEM images of working electrode of bare SPCE (A), CS/SPCE (B) and AuNPs/CS/SPCE (C) with magnification of 50 KX. (D) The CV curves of bare SPCE (a) and AuNPs/CS/SPCE (b) in 0.2 M H_2SO_4.

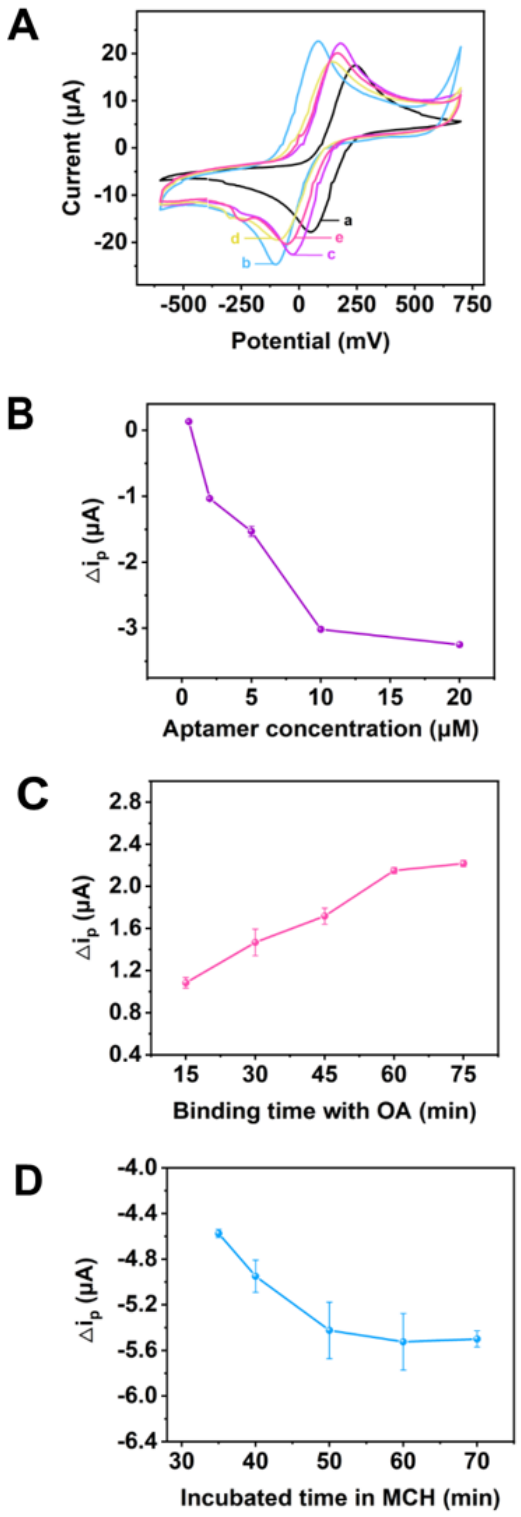

Figure 4

(A) The reduction percentage of reduction peak current in 5 mM $[Fe(CN)_6]^{3-/4-}$ containing 100 mM KCl after exposing in different concentrations of OA including 0.001, 0.01, 0.1, 1, 10, 50 and 100 ng/mL, and its calibration plot for $\Delta i_p/i_{p,0}$ versus Log (concentration). (B) The CV measurements of 10 ng/mL OA of inter-day experiments for five consecutive days in $[Fe(CN)_6]^{3-/4-}$ with 0.1M KCl.

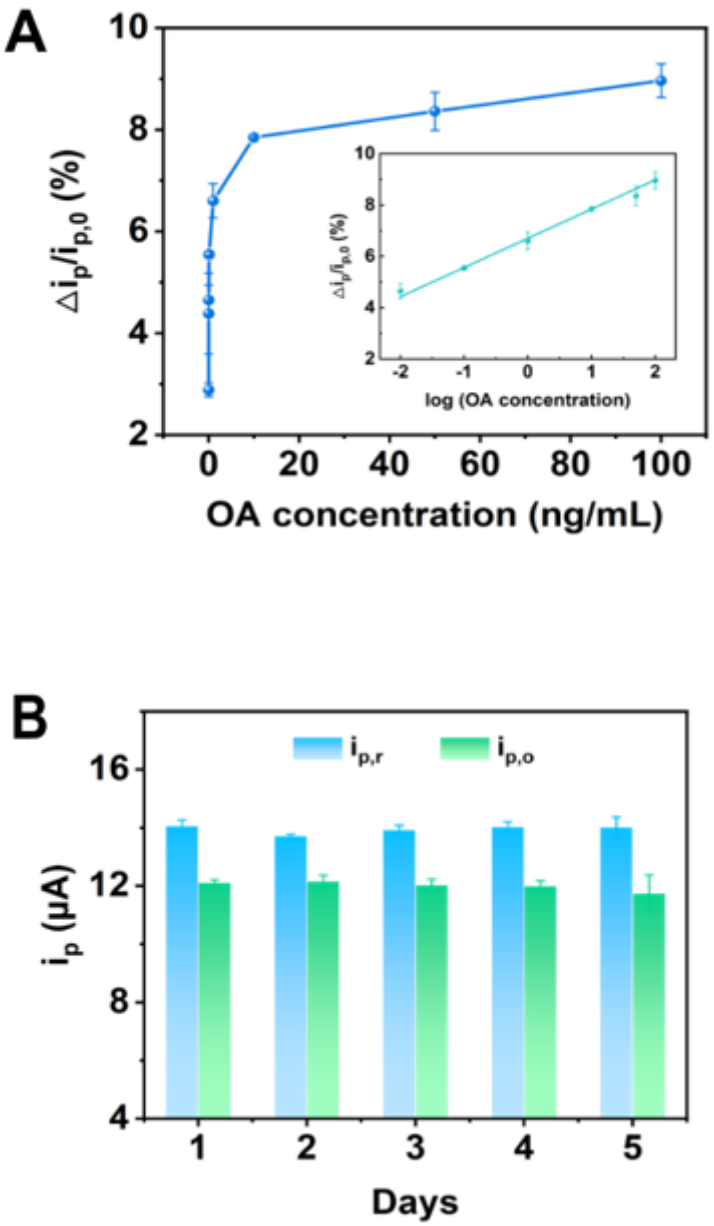

Figure 5

(A) The reduction percentage of reduction peak current in 5 mM [Fe(CN)6]3−/4− containing 100 mM KCl after exposing in different concentrations of OA including 0.001, 0.01, 0.1, 1, 10, 50 and 100 ng/mL, and its calibration plot for Δip/ip,0 versus Log (concentration). (B) The CV measurements of 10 ng/mL OA of inter-day experiments for five consecutive days in [Fe(CN)6]3−/4− with 0.1M KCl.